CHEMICAL ENGINEERING TRANSACTIONS
VOL. 33, 2013
A publication of AIDIC
The Italian Association of Chemical Engineering
Online at: www.aidic.it/cet
Guest Editors: Enrico Zio, Piero Baraldi

ISBN 978-88-95608-24-2; **ISSN** 1974-9791
DOI: 10.3303/CET1333010

Extraction of Gear Fault Feature Based on the Envelope and Time-Frequency Image of S Transformation

Jian Min Liu, Yuan Hong Liu, Jiang Peng Cheng, Fu Zhou Feng*

Department of Mechanical Engineering, Academy of Armored Force Engineering Beijing, No.21, Dujiakan District, Fentai area, Beijing 100072, China.
hong0516@yahoo.com.cn

When a gear has a local fault, the vibration signals of gear may contain amplitude and phase modulation. Their spectrums contain meshing frequencies, harmonics, and coupling frequencies generated by modulation. According to the characteristics of vibration signals from the gears with faults, a feature extraction method of gear fault based on the envelope analysis and time-frequency image of S transformation was proposed. Firstly, vibration signals of wear gears of varying degrees were collected from the fault simulations. Then, envelopes were obtained by Hilbert transform of vibration signals and time-frequency contour maps of envelopes were achieved by S transformation. Finally, the features were extracted by calculating statistics base on the grey-scale matrixes (GLCMs) of the maps. The result shows that the proposed method can effectively extract gear fault feature.

1. Introduction

The key point of condition monitoring and fault diagnosis for gear is fault feature extraction. The ideal vibration signals of normal gear may contain amplitude and phase modulations, and their spectrums include meshing frequencies and harmonics. Gear failures, such as broken teeth, pitting corrosion, wear, etc., will generate periodic pulses in vibration signals, resulting in modulation sidebands on both sides of meshing frequencies and harmonics in the spectrum (Fan and Zuo, 2006).

It is an effective method of gear fault diagnosis to apply the envelope analysis to draw periodic pulse signals. The existing envelope extraction methods mainly include: Hilbert transform demodulation, detector -filtering method, and high-pass absolute value demodulation. The envelope of signal midline is demodulated by high-pass absolute value demodulation method, and the midline envelope of positive half cycle signal is obtained by the demodulation-filter method. The two methods above cannot get the real amplitude of the envelope. However, the envelope of signal of absolute value is acquired by the Hilbert transform, the demodulated amplitude of which represents the true envelope (Lin, Liu and Qu, 1998).

The S-transform advanced by R.G. Stockwell and his colleagues is an important tool in recent years for study of the time-frequency distributions of signals (Stockwell, Mansinha, and Lowe, 1996). The S transform is unique in that it adopts scalable Gaussian window provides resolution related to frequency, which can be used to detecting harmonic signals availably (Cheng, Ling, Wei and Li, 2007). The inverse frequency dependence of the localizing Gaussian window is an improvement over the fixed width window used in the STFT (, Xu , Hao , Jia, and Jing, 2008). The phase of the S transform referenced to the time origin offers useful and supplementary information about spectrum that is not available from locally referenced phase information in the wavelet transform. Since the S transform is a linear time-frequency conversion, there is no cross-term that is inevitable in quadratic time-frequency transform, such as Wigner Ville distribution (Yang, Zhou and Zhang, 2010). The S transform-based time-frequency analysis method has been widely used in recent years in the field of seismic signal processing (Pinnegar and Mansinh, 2003), medical signal processing (Pinnegar, Houman and Federico, 2009), power technology (Zhao and Yang, 2007), etc. Image features primarily consist of the statistical characteristics of color or gray scale, texture, edge features, characteristics of transform coefficients and algebraic characteristics. The time-frequency distribution contour map of vibration signal envelope reflects the texture mostly along direction

Please cite this article as: Liu J.M., Liu Y.H., Cheng J.P., Feng F.Z., 2013, Extraction of gear fault feature based on the envelope and time-frequency image of s transformation, Chemical Engineering Transactions, 33, 55-60 DOI: 10.3303/CET1333010

of the frequency and the time axes, which is sensitive to deformation, for instance, translation, rotation. Haralick proposed fourteen kinds of statistics based on the gray level co-occurrence matrixe(GLCM), which can effectually represents image texture features(Haralick et al., 1973).

The paper combined envelope analysis with the time-frequency image of S transformation to extract the fault features according to the traits of gear vibration signal. Firstly, envelopes were obtained by Hilbert transform. Then, time-frequency images of envelopes were achieved by S transform. Finally, the features were collected by GLCMs and their statistics.

2. Hilbert transform

Model of gear vibration signal of a single frequency modulation is expressed as:

$$x_m(t) = x_m[1 + A_m \cos(2\pi f_n t)]\cos(2\pi m f_z t) \tag{1}$$

Where, x_m is the amplitude of the m-th order harmonic component of meshing frequency, and A_m is the amplitude of the m-th order component of the amplitude modulation function. f_n is the rotation frequency of the gear shaft, and f_z is the gear meshing frequency carrier component. The Hilbert transform is defined by(Michael, 2011):

$$\hat{x}_m(t) = \frac{1}{\pi}\int_{-\infty}^{+\infty}\frac{x_m(\tau)}{t-\tau}d\tau = x_m[1 + A_m \cos(2\pi f_n t)]\sin(2\pi m f_z t) \tag{2}$$

The envelope of the analytical signal $z_m(t)$ is obtained as follows:

$$\left|z_m(t)\right| = \left|x_m(t) + j\hat{x}_m\right| = \sqrt{x_m^2(t) + \hat{x}_m^2(t)} = x_m\left|1 + A_m \cos(2\pi f_n t)\right| \tag{3}$$

3. S transform

The continuous S transform of the signal x(t) is as follows (Tang, Teng, Gao and Zhou, 2012):

$$S(\tau,f) = \int_{-\infty}^{+\infty} x(t)\omega(t-\tau,f)e^{-i2\pi ft}dt, \quad \omega(t-\tau,f) = \frac{|f|}{\sqrt{2\pi}}e^{-\frac{(\tau-t)^2 f^2}{2}} \tag{4}$$

$\omega(t-\tau,f)$ is a Gaussian window function. τ is the last shift factor, and f is the frequency. Let $\tau = mT_s, f = k/NT_s$, the one-dimensional discrete transform of $x(nT_s)$ is:

$$S(mT_s, k/NT_s) = \sum_{r=0}^{N-1} X\left[\frac{r+k}{NT_s}\right]G(r,k)e^{\frac{j2\pi mr}{N}}, k \neq 0, \quad S(mT_s,0) = \sum_{r=0}^{N-1} X\left(\frac{r}{NT_s}\right), k = 0 \tag{5}$$

$$X\left(\frac{k}{NT_s}\right) = \frac{1}{N}\sum_{n=0}^{N-1} x(nT_s)e^{-i2\pi kn/N} \qquad G(r,k) = e^{-2\pi^2 r^2/k^2} \tag{6}$$

k, m, n is the sampling points in the range [0, N-1]. T_s is the sampling interval. $X(r/NT_s)$ is the discrete Fourier transform of the signal $x(nT_s)$. $G(r,k)$ is a Gaussian window function of Fourier spectrum. Thus discrete S transform can be realized by fast Fourier transform of the discrete signal $x(nT_s)$, and the number of operations of S transform for one point is the same with the FFT.

4. The GLCM theory

4.1 GLCM

The GLCM shows the occurrence probability of two pixels of certain distance and direction in a picture (Bai, Wang and Wang, 2005). Supposing that locations of two pixels in an image are (x_1, y_1) and (x_2, y_2), and the gray-scale values corresponding with them are *i* and *j* respectively. Then the GLCMs $P_{0°}$, $P_{45°}$, $P_{90°}$and $P_{135°}$of four different directions, 0°, 45°, 90° and 135° are obtained for a given distance d, which is detailedly specified in reference.

4.2 Statistics based on GLCM

We select six of all the fourteen kinds of statistics based on GLCM put forward by Haralick in our study to quantitatively evaluate textural parameters, which are often used in characteristic extraction of image texture. The following equations define these features. Let $p(i,j,d,\theta)$ be $i,j)$ th entry in a normalized GLCM, The mean and standard deviations for the rows and columns of the matrix are

$$u_x = \sum_i \sum_j i \cdot p(i,j,d,\theta) \qquad \sigma_x = \sum_i \sum_j (i-u_x)^2 p(i,j,d,\theta)$$
$$u_y = \sum_i \sum_j j \cdot p(i,j,d,\theta) \qquad \sigma_y = \sum_i \sum_j (j-u_y)^2 p(i,j,d,\theta) \tag{7}$$

The features are computed as follows. g is the number of distinct gray levels in the quantized image.

1) Energy:

$$f_1 = \sum_{i=1}^{g} \sum_{j=1}^{g} p^2(i,j,d,\theta) \tag{8}$$

2) Contrast:

$$f_2 = \sum_{i=1}^{g} \sum_{j=1}^{g} (i-j) p^2(i,j,d,\theta) \tag{9}$$

3) Correlation:

$$f_3 = \frac{\sum_{i=0}^{g-1} \sum_{j=0}^{g-1} (i \times j \times p(i,j,d,\theta)) - u_x \times u_y}{\sigma_x \times \sigma_y} \tag{10}$$

4) Entropy:

$$f_4 = -\sum_{i=1}^{g} \sum_{j=1}^{g} p(i,j,d,\theta) \log_{10} p(i,j,d,\theta) \tag{11}$$

5) Variance:

$$f_5 = \sum_{i=1}^{g} \sum_{j=1}^{g} (i-u)^2 p(i,j,d,\theta) \tag{12}$$

6) Inverse Difference Moment:

$$f_6 = \sum_{i=0}^{I-1} \sum_{j=0}^{I-1} p(i,j,d,\theta) / (1+(i-j)^2) \tag{13}$$

5. The acquisition of gear vibration signals

The research object is a transmission applied in the vehicle BJ2020S. The diagram of gearbox structure is shown as Figure 1. The simulant wear fault was executed by fraying the normal gear Z_6 in the output shaft.

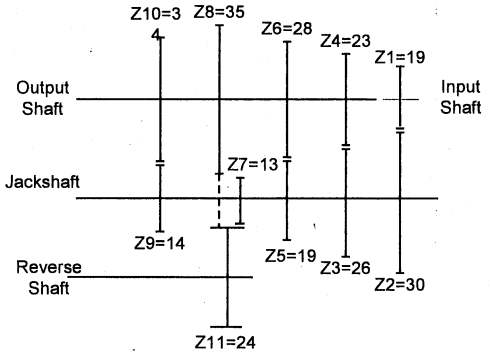

Figure 1: The diagram of gearbox structure

The simulant experiment was carried out on the test bench, where the output shaft of the DC motor was connected to the input shaft of the transmission, and the output shaft of the transmission was connected to the load adjusting device (DC generator), while the optoelectronic speed sensor was used to get the accurate speed of the motor output shaft. The acceleration sensor was placed in surface of the transmission near to the radial way of output shaft to pick up the vibration acceleration signal, when the transmission was rotating in second gear.

The sampling frequency was set to 10 kHz, and sampling points N = 20,000, thus, the frequency resolution. $\Delta f = f_s / N = 0.5Hz$ The collected gear vibration signals of normal, slight wear and severe wear after normalization processing are shown in Figure 2. The real rotating speeds of motor output shaft measured by the optoelectronic speed sensor were 617.6 r/min, 609.2 r/min and 620r/min, when the rotational speed was set to 630 r/min by the motor controller. Therefore, the exact rotation frequencies of the output shaft with gear of different wears can be calculated by the following formula.

$$f_n = n \times Z_1 / 60 / Z_2 \times Z_5 / Z_6 \qquad (14)$$

The frequencies are 4.42 Hz, 4.36Hz and 4.44Hz separately for n=617.6 r/min, 609.2 r/min and 620r/min

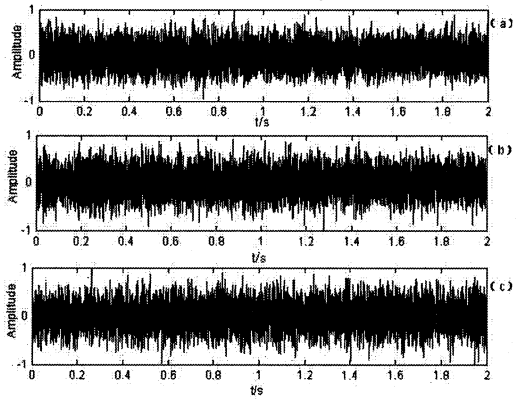

Figure 2: Normalized vibration signals of the transmission. (a) normal (b) slight wear (c) severe wear

6. Features extraction of gear fault

Firstly, use the Hilbert transform to the Gear vibration signals in Figure 2 to gain the envelope signals. Then, it is necessary to resample the envelope signals to reduce the number of operations by S transform and not to change the frequency resolutions of envelope signals. To prevent frequency aliasing, it is obligatory to apply the Butterworth low-pass filter to filter the envelope signals before resampling. The filter order is set to 10, the cutoff frequency 1000Hz, and the re-extracting multiple $D = 10$. Then, the sample frequency after resampling is $f_s^{'} = f_s / D = 10000/10 = 1000\text{Hz}$, and the sample number is $N = 2000$. When the gears in output shaft are differently attrited, the periodic pulses are mixed with the vibration signals, which leads to the emergence of rotation frequencies and their harmonics in the spectrums. The strength of pulse signals are varying as the wear degree changes, resulting in the unclear differences in the high order frequency multiplications of rotation frequencies. Therefore, the analysis frequency is selected to 20Hz, slightly greater than four times rotation frequency of the output shaft. The sampling time is initialized to 2s. Then, the time required for S transform is 0.04186s before resampling, and the time required only 0.005731s after resampling. The gray contour maps of time-frequency images by S transform of envelope signals are shown in Figure 3. The size of which is 462x364 pixels, and the gray level 256. Figure 3 shows the image texture with normal gear is the most detailed, while the texture with gear of severe wear is the most rough.

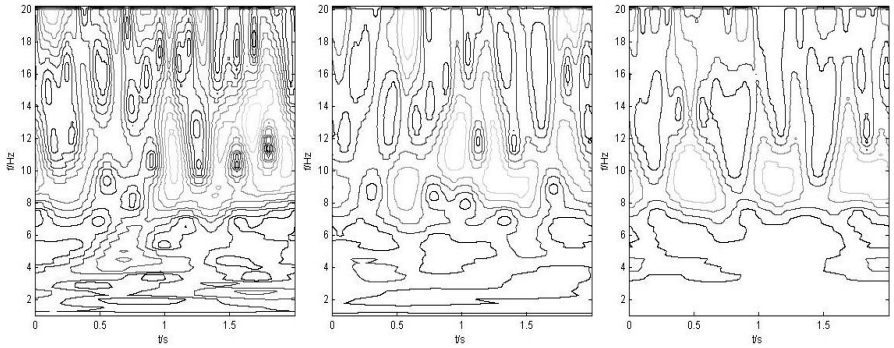

(a) normal (b) slight wear (c)severe wear

Figure 3: The contour maps of envelope S Transformation time-frequency Image of gear vibration signal

In order to abate the random interference in vibration signals and extract the features effectively, it is essential to gather multi groups of vibration signals to average the statistics. Five groups of vibration signals of gears of different wears were gathered in the experiments. The time-frequency images of S transform of envelope signals are obtained, and the sizes of contour maps of which are the same as maps in Figure 3. According to traits of simplex and small texture, Let d=1, then compute the GLCMs, based on which the average statistics for normal, slight wear and severe wear gear are achieved, shown in Table 1, Table 2 and Table 3.

Table1 The eigenvalues of time-frequency contour maps of envelope signals from normal gear

Features	0°	45°	90°	135°
Energy	0.682128	0.629803	0.677777	0.628965
Contrast	4019.887	6804.936	4533.621	6857.899
Correlation	0.48943	0.111331	0.403861	0.102188
Entropy	0.413889	0.471497	0.426777	0.471941
Variance	1.04E-05	9.61E-06	1.03E-05	9.6E-06
Inverse Difference Moment	0.884409	0.807558	0.872292	0.806817

Table 2 The eigenvalues of time-frequency contour maps of envelope signals from gear of slightly wear

Features	0°	45°	90°	135°
Energy	0.7283898	0.690741	0.7389701	0.690938
Contrast	3775.1098	6024.553	3852.7942	6015.446
Correlation	0.46261705	0.122889	0.439277	0.124825
Entropy	0.34787431	0.384222	0.3392996	0.384115
Variance	1.1114E-05	1.05E-05	1.128E-05	1.05E-05
Inverse Difference Moment	0.89768635	0.847274	0.9057324	0.847505

Several conclusions can be drawn from the tables above, as follows.

(1) The correlation values in directions of $\theta = 0^0, 90^0$ are obviously larger than that in directions of $\theta = 45^0, 135^0$, when the gears are of different wears (normal, slight wear, severe wear), which shows that the major texture directions of contour maps are along the time axis and frequency axis. Moreover, the correlation values in direction of $\theta = 0^0$ are the biggest, when the gears are normal or slight wear. That is, the central texture direction is along the time axis. Accordingly, the main direction is along the frequency axis, when the gear is of severe wear.

Table 3 The eigenvalues of time-frequency contour maps of envelope signals from gear of heavy wear

Features	0°	45°	90°	135°
Energy	0.75342317	0.717892	0.762514	0.719981
Contrast	3599.91109	5627.284	3498.164	5496.322
Correlation	0.45713431	0.130321	0.460556	0.153085
Entropy	0.31859152	0.354273	0.312724	0.353077
Variance	1.1496E-05	1.1E-05	1.16E-05	1.1E-05
Inverse Difference Moment	0.90851396	0.860812	0.914301	0.863256

(2) The values of the remained statistics with $\theta = 0^0, 45^0, 90^0, 135^0$ of the contour maps change with the increase in the degree of gear wear. The values of contrast and entropy decrease in turn, while the values of energy, inverse difference moment and variance in turn increases, which perform the gear fault feature perfectly. So the statistics can serve as the gear fault characteristic parameters.

7. Conclusions

(1) The paper combined the vibration signal envelope with S transform to extract gear fault features. The results show that the characteristic parameters respond to the varying conditions of gear stably.
(2) To put the proposed method into practice of the condition monitoring and fault diagnosis of gear, it is necessary to resample the envelope signal to reduce the number of operations of the S transform for one point. In order to prevent frequency aliasing, low pass filter should be employed prior to the extraction of the envelope signal. Moreover, it is necessary to normalize the parameters before classification to implement identification and classifications of gear conditions in condition monitoring and fault diagnosis effectively by the gear fault characteristic parameters.

References

Bai X.B., Wang K.Q., Wang H.,2005, Research on the classification of wood texture based on Gray Level Co- occurrence Matrix, JOURNAL OF HARBIN INSTITUTE OF TECHNOLOGY, 37(12), 1667-1670

Cheng Z.Y., Ling D., Wei S., Li L.D., 2007, Dynamic detection of inter-harmonics based on S-transform, Electrical Measurement & Instrumentation, 44(495), 998-1001.

Fan X.F., Zuo M.L., 2006, Gearbox fault detection using Hilbert and wavelet packet transform, Mechanical Systems and Signal Processing, 20(4), 966-982.

Haralick R.M., Shanmugam K., Dinsteein I.,1973, Texture features for image classification, IEEE Trans on System, Man and Cybernetics, 8(6),610-621.

Lin J., Liu H.X., Qu L.S., 1998, Envelope Characteristic Recognition and Its Application in Mechanical Fault Diagnosis, Journal of Vibration, Measurement & Diagnosis, 18(3), 34-48.

Michael F., 2011, Hilbert transform in vibration analysis, Mechanical Systems and Signal Processing, 25(3), 735-802.

Pinnegar C R, Mansinh A L., 2003, The S-transform with windows of arbitrary and varying shape, Geophysics, 68(1), 381-385.

Pinnegar C.R., Houman K., Federico P., 2009, Time–Frequency Phase Analysis of Ictal EEG Recordings With the S-Transform, IEEE Transactions on Biomedical Engineering, 56(11), 2583-2593.

Stockwell R.G., Mansinha L., Lowe R.P., 1996, Localization of the Complex Spectrum: The S Transform, IEEE Transactions on Signal Processing, 44(4), 998-1001.

Tang Q., Teng Z.S., Gao Y.P., Zhou Y.B., 2012, Voltage Flicker Measurement Using Square Demodulation Method Based on S-transform, Proceedings of the CSEE, 32(7), 60~67.

Xu H.M., Hao Z.Y., Jia W.X. Jing G.X., 2008, Study on Vibration Characteristics of Internal Combustion Engine Cylinder Head Based on S Transform, Chinese Internal Combustion Engine Engineering, 29(3), 68-75.

Yang X.Y., Zhou X.J., Zhang W.B, 2010, Rolling bearing fault feature extraction based on morphological wavelet and S-transform, Journal of Zhejiang University (Engineering Science), 44(11), 2088-2093.

Zhao F.Z., Yang P.G., 2007, Power-Quality Disturbance Recognition Using S-Transform, IEEE Transactions on Power Delivery, 22(2), 944-950.